United States Department of Agriculture | **Natural Resources Conservation Service** | **5 Radnor Corporate Center, Suite 200 Radnor, PA 19087-4585**

Subject: SOI -- Geophysical Assistance -- **Date:** 1 October 1996

To: Liana E. Kier
State Conservationist
USDA-NRCS,
3244 Elder Street
Boise, Idaho 83705

PURPOSE:

The purpose of this investigation was to use electromagnetic induction (EMI) and ground-penetrating radar (GPR) techniques to characterize fragipans in areas of Santa and Reggear soils.

PARTICIPANTS:

Jim Doolittle, Research Soil Scientist, USDA-NRCS, Radnor, PA
Mary Doolittle, Earth Team Volunteer, USDA-NRCS, Radnor, PA
Anita Feller, University of Idaho, Moscow, ID
Brian Gardner, Soil Scientist, ISCC, Orofino, ID
Glenn Hoffmann, Soil Survey Party Leader, USDA-NRCS, Orofino, ID
Paul McDaniel, Professor of Soil Science, University of Idaho, Moscow, ID
Neil Peterson, State Soil Specialist, USDA-NRCS, Boise, ID
Shaney Rockefeller, Graduate Student, University of Idaho, Moscow, ID
Brad Rust, Soil Scientist, USDA-NRCS, Orofino, ID
Hal Swenson, Soil Scientist, USDA-NRCS, Boise, ID
Sara Young, Graduate Student, University of Idaho, Moscow, ID

ACTIVITIES:

All field activities were completed during the period of 29 July to 1 August 1996.

EQUIPMENT:

The radar unit used in this study was the Subsurface Interface Radar (SIR) System-2, manufactured by Geophysical Survey Systems, Inc.[1] The SIR System-2 consists of a digital control unit (DC-2) with keypad, VGA video screen, and connector panel. The principal antenna used in this investigation was the model 3105 (300 mHz). The system was powered by a 12-volt battery. This unit is backpack portable and requires two people to operate. The use and operation of GPR have been discussed by Morey (1974), Doolittle (1987), and Daniels and others (1988).

The electromagnetic induction meters used in this study were the EM38 and EM31, manufactured by Geonics Limited.[1] These meters are portable and require only one person to operate. Principles of operation have been described by McNeill (1980a, 1986). No ground contact is required with these

[1] Trade names have been used in this report to provide specific information. Their use does not constitute endorsement.

meters. Each meter provides limited vertical resolution and depth information. For each meter, lateral resolution is approximately equal to the intercoil spacing. The observation depth of an EMI meter is dependent upon intercoil spacing, transmission frequency, and coil orientation relative to the ground surface.

To help summarize the results of this study, the SURFER for Windows software program developed by Golden Software Inc. was used to construct two- and three-dimensional simulations.[2] Grids were created using kriging methods with an octant search. All grids were smoothed using a cubic spline interpolation. In each of the enclosed plots, shading and filled contour lines have been used. These options were selected to help emphasize spatial patterns. Other than showing trends and patterns in values of apparent conductivity (i.e., zones of higher or lower electrical conductivity) or estimated depths to fragipans, no significance should be attached to the shades themselves.

STUDY SITE:

The sites were located in Latah and Clearwater counties, Idaho (see Figure 1). Two sites were located near the town of Troy in Latah County. These sites are being monitored by Shaney Rockefeller and Sara Young. One site was located entirely in an open field. This site will be referred to as the *Troy site*. The other site consisted of two plots, one in an open field and the other in an adjoining forested area. This site will be referred to as the *Santa site*. Both sites were located in areas of Santa soil. Santa soils are members of the coarse-silty, mixed, frigid, Ochreptic Fragixeralfs family. These very deep, moderately-well drained soils formed in loess on uplands. Santa soils are moderately deep to a fragipan.

The site in Clearwater County was located near the town of Weippe. This site is being monitored by Shaney Rockefeller. The site consisted of two plots, one in an open field and the other in an adjoining forested area. This site was located in areas of Reggear soil and will be referred to as the *Reggear site*. Reggear soils are members of the fine-silty, mixed, Vitrandic Fragiboralfs family. These very deep, moderately-well drained soils are on uplands. Reggear soils formed in a thin mantle of volcanic ash, loess, and alluvium over lacustrine sediments. Reggear soils are moderately deep to a fragipan.

FIELD PROCEDURES:

Rectangular grids were established across each site. Grid intervals ranged from 5 to 15 m. A survey flag was inserted in the ground at each grid intersection and served as an observation point. At each observation point, the relative elevation of the surface was determined with a level and stadia rod. Elevations were not tied to a benchmark; the lowest observation point within each site served as datum (0.0 m).

At each observation point, measurements were taken with an EM38 meter in both the horizontal and vertical dipole orientations. For each measurement, the meter was placed on the ground surface. The radar survey was completed by pulling the 300 mHz antenna along one set of parallel grid lines. Although, GPR provides a continuous profile of subsurface conditions, interpretations of the depths to fragipan were restricted to the observation points.

DISCUSSION:

Ground-penetrating Radar:

Ground-penetrating radar is an impulse radar system designed for shallow (0 to 30 m), subsurface investigations. This system operates by transmitting short pulses of high frequency (10-1000 mHz) electromagnetic energy into the ground from an antenna. Each pulse consists of a spectrum of frequencies distributed around the center frequency of the transmitting antenna. Whenever a pulse

[2] Trade names have been used to provide specific information. Their use does not constitute endorsement,

contacts an interface separating layers of differing electromagnetic properties, a portion of the energy is reflected back to the receiving antenna. The receiving unit amplifies and samples the reflected energy, and converts it into a similarly shaped waveform in a lower frequency range. The processed reflected waveforms can be displayed on a VGA video screen, printed on a thermal recorder, or stored on an internal disk drive for future playback and/or post-processing.

Most diagnostic subsurface horizons used to classify soils within the United States have been charted with GPR. These horizons often have abrupt upper boundaries which contrast with overlying horizons in physical (texture, bulk density, moisture) and chemical (organic carbon, calcium carbonate, sesquioxide contents) properties. Typically, these interfaces produce strong reflections and distinct GPR imagery. Ground-penetrating radar has been used to estimate depths to soil horizons (Collins and Doolittle, 1987; Doolittle, 1987; Doolittle and Asmussen, 1992), hard pans (Olson and Doolittle, 1985), dense till (Collins et al., 1989), and permafrost (Doolittle et al., 1990 and 1992). It has been used to infer soil color or organic carbon content (Collins and Doolittle, 1987); assess the continuity of ortstein (Mokma et al., 1990a) determine thickness of organic soil materials (Shih and Doolittle, 1984; Collins et al., 1986); chart the depths to relatively shallow (< 12 m) water tables in predominantly coarse textured soils (Shih et al., 1986); assess the concentration of lamellae in soils (Farrish et al., 1990; Mokma et al., 1990b); and evaluate the thickness of surface (Doolittle, 1987) and active layers (Doolittle et al. 1990). Radar interpretations have provided transect data for soil survey reports (Doolittle, 1987; Collins et al., 1986; Schellentrager et al., 1988; and Puckett et al., 1990). In addition, GPR has been used to study changes in soil properties that affect forest productivity (Farrish et al., 1990) and stress in citrus trees (Shih et al., 1985).

In some soils, the use of GPR is inappropriate. Because of high electrical conductivity, some soils are essentially radar opaque. In these soils, observation depths are limited and resolution of subsurface features is often poor. In some instances, the depth of observation can be extended by using multiple arrays, closely spaced borehole antennas, or relying on signal processing methods. However, these techniques do not guarantee results and are more expensive and time consuming than surface approaches.

Ground-penetrating radar is a time scaled system. This system measures the time that it takes electromagnetic energy to travel from the antenna to an interface (e.g., soil horizon, stratigraphic layer, bedrock surface) and back. To convert the travel time into a depth scale, either the velocity of pulse propagation or the depth to a reflector must be known. The relationships among depth (d), two-way, pulse travel time (t), and velocity of propagation (v) are described in the following equation (Morey, 1974):

$$v = 2d/t$$

The velocity of propagation is principally affected by the relative permittivity or dielectric constant (e) of the profiled materials according to the equation:

$$e = (c/v)^2$$

Where c is the velocity of propagation in a vacuum (0.3 m/nanosecond). A nanosecond (ns) is one billionth of a second. The amount and physical state of water (temperature dependent) have the greatest effect on the dielectric constant of a material. Tabled values are available that approximate the dielectric constant of some materials (Morey, 1974; Petroy, 1994). However, as discussed by Daniels and others (1988), these values are simply approximations.

Calibration trials were conducted within the Troy and Reggear sites. The purposes of the calibration trials were to determine the dielectric constant and velocity of propagation of electromagnetic energy through the soil. These values were used to establish depth scales. The calibration trials afforded an opportunity to optimize control and recording settings and to verify interpretations. During these trials,

traverses were conducted with the 500, 300, and 120 MHz antennas. The 300 mHz antenna provided the most acceptable balance of resolution and depth of observation. Considerations of desired versus achievable depths of observation and the resolution of subsurface features influenced the selection of scanning times. A scanning time of 50 nanoseconds was used during calibration and in all subsequent field work.

Metallic reflectors were buried in the ground at each calibration site. The depths to the tops of these reflectors were 50 cm and 40 cm at the Troy and Reggear sites, respectively. Based on the round-trip travel time to the buried reflector, the averaged velocity of propagation through the Santa soil (Troy Site) was estimated to be 0.123 m/ns. The dielectric constant of the surface layers of Santa soil was estimated to be 5.98. The averaged velocity of propagation through the Reggear soil (Reggear Site) was estimated to be 0.102 m/ns. The dielectric constant of the surface layers of Reggear soil was estimated to be 8.65. At both sites, estimated values were within the range of table values reported by Petroy (1994) for silty materials (e = 5 to 30; v = 0.05 to 0.13 m/ns). Based on estimated velocities of propagation, the scanning time of 50 ns would provide maximum observation depths of about 3.1 and 2.6 m in areas of Santa and Reggear soils, respectively.

Figure 2 is an example of a radar profile. The horizontal scale represents units of distance traveled along an antenna traverse. This scale is dependent upon the speed of antenna advance along a traverse line and the rate of paper advance through the thermal plotter. The vertical scale is a time or depth scale that is based on the velocity of signal propagation.

The four basic components of a radar profile have been identified in Figure 2. These components are the start of scan pulse (A), inherent antenna noise (B), surface reflection (C), and subsurface reflections (D). Except for the start of scan pulse, each of these components is generally displayed as a group of dark bands. The number of bands can be limited by high rates of signal attenuation or superimposed signals. The widths of these bands limit the resolution of closely spaced interfaces. The dark bands occur at both positive and negative signal amplitudes. The narrow white band(s) separating the darker bands represent the neutral or zero crossing between positive and negative signal amplitudes.

The start of scan pulse (see A in Figure 2) results from direct feed-through of transmitted pulses into the receiver. Though a source of unwanted clutter, the start of scan pulse is often used as a time reference line.

Reflections unique to each of the system's antennas are the first series of multiple bands on radar profiles (see B in Figure 2). Generally the width of these bands increases with decreasing antenna frequency or signal filtration. These reflections are a source of unwanted noise on radar profiles.

The surface reflection (see C in Figure 2) represents the surface of the soil. Below the surface reflection are reflections from subsurface interfaces (see D in Figure 2). Interfaces can be categorized as being either *plane* or *point reflectors*. Most soil horizons and geologic strata appear as a series of continuous, parallel bands similar to those appearing in the left-hand portion of Figure 2. Features that produce these reflections are referred to as *plane reflectors*. Small objects such as rocks, roots, or buried cultural features can produce a hyperbolic pattern similar to the feature appearing in the right-hand portion of Figure 2. Features that produce these reflections are referred to as *point reflectors*.

Computer processing of radar imagery is relatively expensive, time consuming, and not justified for all radar surveys (Violette, 1987). However, in some studies, the processing of radar imagery has enhanced the resolution of subsurface features and reduced interpretation errors. The radar profiles shown in this report have been processed through RADAN software. Processing was limited to signal stacking, normalization of horizontal and vertical scales, and annotations. Arcone (1982) observed that signal stacking reduces incoherent background noise while enhancing the images of subsurface reflectors. Often, because of noise suppression, stacked traces have considerably more discernible features especially at greater depths. Normalizing the horizontal scale adjusts for differences in the

speed of antenna advance across the ground surface. Normalizing the vertical scale is often referred to as *terrain correction*. Terrain correction is a process whereby the surface of the radar profile is adjusted to conform more closely to the surface topography. At each grid intersection, the radar profiles have been adjusted to the elevation of the ground surface. Only the radar profiles from the Troy site have been terrain corrected.

Electromagnetic Induction:

Electromagnetic induction uses electromagnetic energy to measure the apparent conductivity of earthen materials. Apparent conductivity is a weighted average conductivity measurement for a column of earthen materials to a specified observation depth. Variations in apparent conductivity are produced by changes in the electrical conductivity of earthen materials. The electrical conductivity of soils is influenced by the (i) volumetric water content, (ii) type and concentration of ions in solution, (iii) temperature and phase of the soil water, and (iv) amount and type of clays in the soil matrix, (McNeill, 1980b). The apparent conductivity of soils increases with increases in the exchange capacity, water and clay contents. Values of apparent conductivity are seldom diagnostic in themselves, but lateral and vertical variations in these measurements can be used to infer changes in soils and earthen materials. Interpretations of the EMI data are based on the identification of spatial patterns within data sets.

Advantages of EMI methods include speed of operation, flexible observation depths (with commercially available systems from about 0.75 to 60 meters), and moderate resolution of subsurface features. Results of EMI surveys are interpretable in the field. These methods can provide in a relatively short time the large number of observations needed for site characterization and assessments. Maps prepared from correctly interpreted EMI data provide the basis for assessing site conditions and for planning further investigations.

Like GPR, EMI techniques are not suitable for use in all soil investigations. Generally, the use of EMI techniques has been most successful in areas where subsurface properties are reasonably homogeneous and the effects of one property (e.g., clay, water, or salt content) dominate over the other properties. In these areas, variations in EMI response can be related to changes in the dominant property or feature (Cook et al., 1989).

Soil scientists have used EMI techniques extensively to identify, map, and monitor soil salinity (Cook and Walker, 1992; Corwin and Rhoades, 1982, 1984, and 1990; Rhoades and Corwin, 1981; Rhoades et al., 1989; Slavich and Petterson, 1990; Williams and Baker, 1982; and Wollenhaupt et al., 1986). Recently, the use of this technology has been expanded to include the assessment and mapping of sodium-affected soils (Ammons et al., 1989; Nettleton et al., 1994), depths to claypans (Sudduth and Kitchen, 1993; Doolittle et al., 1994), and edaphic properties important to forest site productivity (McBride et al., 1990).

Variations in apparent conductivity can be used to infer changes in soils and soil properties. As EMI measurements integrate the bulk physical and chemical properties for a defined observational depth into a single value, responses have been associated with changes in soils and soil map units (Hoekstra et al., 1992; Jaynes et al., 1993, Doolittle et al., 1996). Jaynes (1996) demonstrated that maps prepared from EMI measurements provided more detailed information than contained in published soil survey reports. For each soil, the inherent variability in physical and chemical properties, as well as temporal variations in soil water and temperature, will establish a characteristic range of observable apparent conductivity values. This range is influenced by differences in use or management practices (Sudduth and Kitchen, 1993).

Two EMI meters were used in this study. The EM38 meter has a fixed intercoil spacing of about 1 meter. It operates at a frequency of 13.2 kHz. Theoretically, the EM38 meter has observation depths of about 75 and 150 centimeters in the horizontal and vertical dipole orientations, respectively (McNeill,

1986). The EM31 meter has a fixed intercoil spacing of about 3.65 meters. It operates at a frequency of 9.8 kHz. Theoretically, the EM31 meter has observation depths of about 3 and 6 meters in the horizontal and vertical dipole orientations, respectively (McNeill, 1980a). Values of apparent conductivity are expressed in milliSiemens per meter (mS/m).

RESULTS:

Troy Site:

A rectangular grid was established across the site. The grid intervals were 10 and 15 meters. These intervals provided eighty grid intersections or observation points. At each observation point, measurements were taken with an EM38 and an EM31 meter in both the horizontal and vertical dipole orientations. For measurements, each meter was placed on the ground surface.

The topography of the Troy site is shown in Figure 3. In this plot, the contour interval is 2 m. Relief is 19.85 meters. Surfaces slope away from a ridge summit located along the southern boundary of the site. Slope curvatures are complex. The site is characterized by convex slopes with both concave and convex contours. A drainageway is located near and closely parallels the northern borders of the site.

Basic statistics for the EMI data collected within the Troy site are displayed in Table 1. In general, values of apparent conductivity increased and became slightly more variable with increasing observation depths. One negative response (-20 mS/m) was obtained with the EM38 meter in the horizontal dipole orientation. This measurement was presumed to reflect the presence of a cultural feature (buried cable, farm implement).

Table 1

Basic Statistics
EMI Survey
Troy Site
(All values are in mS/m)

				Quartiles			
Meter	Orientation	Minimum	Maximum	1st	Median	3rd	Average
EM38	Horizontal	-20.0	18.4	9.0	10.8	12.7	10.85
EM38	Vertical	9.8	27.6	13.8	15.5	19.1	16.71
EM31	Horizontal	12.3	23.3	15.7	17.1	18.9	17.46
EM31	Vertical	20.4	34.9	24.5	27.5	30.4	27.91

Figures 4 and 5 represent the spatial distribution of apparent conductivity for the upper 0.75 meter and the upper 1.5 meters of the soil profile, respectively. In each plot, the isoline interval is 4 mS/m. Values of apparent conductivity increased slightly with increasing observation depths. Measurements averaged 10.85 mS/m and 16.71 mS/m in the horizontal and vertical dipole orientations, respectively. For the shallower-sensing horizontal dipole orientation, one-half of the observations had measurements between 9 and 12.7 mS/m. For the deeper-sensing vertical dipole orientation, one-half of the observations had measurements between 13.8 and 19.1 mS/m. These vertical trends are believed to reflect increased moisture and clay contents at intermediate and lower soil depths.

Apparent conductivity values were higher in the western portion of the site. In both figures 4 and 5, a line connecting the southwest and the northeast corners would divide the site into two distinct areas. Values of apparent conductivity were generally higher to the west of this line. No explanation for this spatial pattern can be given.

Figures 6 and 7 represent the spatial distribution of apparent conductivity for the upper 3 meters and the upper 6 meters of the soil profile, respectively. In each plot, the isoline interval is 4 mS/m. For these depth intervals, values of apparent conductivity increased with increasing observation depths. Measurements averaged 17.46 mS/m and 27.91 mS/m in the horizontal and vertical dipole orientations, respectively. For the shallower-sensing horizontal dipole orientation, one-half of the observations had measurements between 15.7 and 18.9 mS/m. For the deeper-sensing vertical dipole orientation, one-half of the observations had measurements between 24.5 and 30.4 mS/m. This trend could reflect increased moisture and clay contents at lower soil depths or differences in the parent materials.

As with the plots of the EM38 measurements, in figures 6 and 7, a line connecting the southwest and the northeast corners would divide the site into two distinct areas. Values of apparent conductivity increase towards the west. This trend is more conspicuous in the measurements collected in the vertical dipole orientation (see Figure 7). Again, no explanation for this spatial pattern can be given.

Figure 8 shows the locations of three radar traverses conducted at the Troy site. Along each traverse, the locations of grid intersections or observation points have also been identified. The radar profiles from these traverses are shown in figures 9, 10, and 11. The vertical lines appearing at the top of each radar profile (see figures 9, 10, and 11) represent the locations of grid intersections. Numbers, representing units of distance, have been used to identify these grid intersections.

At the Troy site, the depth of radar observation was restricted to the upper part of the fragipan. High rates of signal attenuation in the surface layers and the upper part of the fragipan limited the depth of observation to less than 1.0 meter.

In each of the radar profiles (figures 9, 10, and 11), the soil surface is represented by two, thin, closely spaced, high and intermediate amplitude lines that extend across the upper part of the profile. The lower of the two lines is lower in amplitude and is discontinuous. Processing and gain settings are responsible for the appearance of the surface reflection. In addition, processing has removed the start of scan pulse and antenna noise.

Immediately below the reflections from the soil surface is a conspicuous, high amplitude reflection. This reflection is a composite image from several closely spaced, surface and near-surface features. These overlapping reflections are poorly resolved because of their shallow range, the antenna and high gain settings used in this survey. These reflections are produced by changes in vegetation, surface roughness, soil texture, horizons, and/or moisture within the upper 25 to 40 cm of the soil profile. These near-surface reflections appear more intense (higher amplitude) on higher-lying slope positions. As these reflections are less intense on lower-lying slope positions, differences are assumed to reflect changes in moisture, texture, and possibly soluble salts. Increases in any one of these factors could dilute the electromagnetic gradients and weaken the reflected signals.

In each figure, the fragipan is believed to be represented by the lowest, visible reflector. Though continuous, this reflector is variable in appearance. The fragipan is represented by a horizontal line of varying amplitudes. In many areas the fragipan consists of multiple, vertical line segments. This graphic signature is unique and could represent reflections from prism faces. The expression of the fragipan changes with slope position. This reflector (the fragipan) is better expressed and more conspicuous on higher-lying slope positions. On these drier slope positions, greater differences in consistency, structure, and/or texture could result in greater reflections of the radar pulse. Typically, the reflection from the fragipan is weaker on lower-lying slope positions. Increased moisture contents would weaken electromagnetic gradients existing between the surface layers and the fragipan. In addition, on moister, lower-lying slope positions, differences in soil consistency between surface layers and the subsoil could be less. This would result in weak electromagnetic gradients and less intense amplitudes of the reflected signals.

In each figure (figures 9, 10, 11), variations in the expression of the fragipan are unique and most intriguing. These patterns could provide soil scientists with insight into the development of fragipans across landscapes.

The radar profile shown in Figure 9 was from the eastern-most traverse shown in Figure 8. In Figure 9, near "A", the fragipan is represented by a very strong, nearly continuous, horizontal reflector. Here, it is presumed that the electromagnetic gradient is abrupt and dielectric properties are strongly contrasting between the surface layers and the fragipan. Because of these properties, the upper boundary of the fragipan produces strong reflections and distinct images in this portion of the radar profile. Near "B" the reflection from the fragipan contains a greater number of vertical line segments. Near "C", the reflection from the fragipan appears to become slightly less intense and is characterized by more widely spaced vertical line segments. The fragipan continues to lose expression (intensity, width, and number of vertical line segments) and deepen slightly across the foot slope (see "E" in Figure 9). The decrease in signal amplitude could indicate increased moisture contents. Increased moisture contents of soils on lower back slope and foot slope positions would be attributed to seepage. Increased moisture will dilute the electromagnetic gradient existing between the surface layers and the fragipan. Lower electromagnetic gradients would produce low amplitude reflections. In Figure 9, a buried point reflector is evident to the left of "F". At "D", a survey flag was passed over by the antenna producing the unique vertical pattern.

Figure 10 is the radar profile from the center line shown in Figure 8. The expression of the fragipan is variable in this profile. Near "A", the fragipan is strongly expressed with numerous, closely spaced vertical line segments. The expression of this layer fades from "B" to "C." Near a drainageway (see "D"), the fragipan, if present, plunges to greater depths. Another, more strongly expressed interface is apparent immediately below "D".

The radar profile shown in Figure 11 is from an area of the site with greater relief and more convex slopes. This profile is from the western-most radar traverse shown in Figure 8. In Figure 11, on areas upslope from "A", the fragipan is represented as a very strong, nearly continuous reflector. Here, soils are drier than on lower slope positions. Therefore, it was assumed that the electromagnetic gradients are more abrupt and dielectric properties are more strongly contrasting between the surface layers and fragipan. Because of these properties, the upper boundary of the fragipan produces strong reflections and distinct images on this portion of the radar profile. Near "B" reflections from the fragipan become weaker and contain a greater number of vertical line segments. Here, the reflection from the fragipan appears to have lost its horizontal component. Near "C" reflections from the fragipan become stronger, regain their horizontal component, and contain a large number of vertical line segments. The expression of the fragipan weakens on the lower back slope (near "D"). This may indicate seepage and the dilution of the electromagnetic gradient between the surface layers and the fragipan. The fragipan continues to lose expression and becomes deeper across the foot slope ("G" in Figure 11). An exception to this trend can be observed near "E".

In Figure 11, reflections from an albic horizon are believed to be expressed to the left of "A" on either side of "C" and possibly "E". These reflections overlie reflections from the fragipan. If these reflections represent the albic horizon, they are present only in some portions of the traverse (near A, C, and E). Similar reflections can be observed in some portions of the radar traverses shown in figures 9 and 10.

Within the study site, based on interpretations of the radar profiles taken at the 80 observation points, the average depth to the fragipan was 0.73 meter with a range of 0.62 to 0. 84 meters. One-half of the observations had depths to fragipan between 0.69 and 0.76 meters. Figure 12 shows the interpreted depths to fragipan across the Troy site. The isoline interval is 0.1 meter. Errors occur in the interpretation of the radar imagery. Errors in radar depth interpretation were considered small. However, interpreted depths need to be verified with auger observations. Errors in the interpreted depths to the fragipan can be attributed to (i) variations in the velocity of propagation of the radar signal through the surface layers, (ii) slight spatial discrepancies among the sites of radar measurement and probe measurements, and (iii) indistinct or ambiguous images of the fragipan on some portions of radar profiles.

Santa Site:
Two rectangular grids were established across the site. One grid was in a cleared area; one grid was located in a forested area. For each grid, the interval was 5 meters. This interval provided twenty-four intersections or observation points within each study area. At each observation point, measurements were taken with an EM38 meter in both the horizontal and vertical dipole orientations. For each measurement, the meter was placed on the ground surface. At each observation point, the relative elevation of the surface was determined with a level and stadia rod. Elevations were not tied to a benchmark; the lowest observation point served as the 0.0 meter datum.

Basic statistics for the EMI data collected within the Santa site are displayed in Table 2. In both the cleared and forested areas, values of apparent conductivity increased and became more variable with increasing observation depths.

Table 2

Basic Statistics
EMI Survey
Santa Site
(All values are in mS/m)

CLEARED AREA

				Quartiles			
Meter	**Orientation**	**Minimum**	**Maximum**	**1st**	**Median**	**3rd**	**Average**
EM38	Horizontal	10.5	12.2	10.9	11.1	11.4	11.20
EM38	Vertical	14.8	22.0	15.7	16.4	17.4	16.78

FORESTED AREA

				Quartiles			
Meter	**Orientation**	**Minimum**	**Maximum**	**1st**	**Median**	**3rd**	**Average**
EM38	Horizontal	4.8	17.7	6.1	7.4	8.6	7.71
EM38	Vertical	7.6	22.6	10.0	11.7	13.5	12.14

Figure 13 is the topography of the grid located in the cleared area. Relief is 11.02 meters. In general, the surface slopes towards the west. The site is characterized by plane slopes with convex contours. A small knob is apparent near the southwest corner of the study area.

Figures 14 and 15 are two-dimensional plots of the data collected with the EM38 meter in the cleared area. Figures 14 and 15 are simulations based on measurements obtained in horizontal and vertical dipole orientations, respectively. In each plot the interval is 4 mS/m. The spatial patterns appearing in these plots are nondescript. Values of apparent conductivity are relatively invariable across the study area, but do increase and become slightly more variable with increasing observation depths.

In the cleared area, measurements averaged 11.2 mS/m and 16.78 mS/m in the horizontal and vertical dipole orientations, respectively. For the shallower-sensing horizontal dipole orientation, one-half of the observations had values of apparent conductivity between 10.9 and 11.4 mS/m. For the deeper-sensing vertical dipole orientation, one-half of the observations had values of apparent conductivity between 15.7 and 17.4 mS/m. This trend is believed to reflect increased moisture and clay contents at intermediate and lower soil depths.

Figure 16 is a radar profile from the cleared study area of the Santa Site. The vertical lines appearing at the top of the radar profile represent the locations of grid intersections. Numbers, representing units of distance, have been used to identify these grid intersections. Interpreted reflections from the albic horizon (near "A") and the fragipan (above "B") are clearly expressed in this profile. Both features appear constant in depth. The albic horizon appears discontinuous and slightly more variable in expression. The fragipan is represented by a very strong, nearly continuous, horizontal reflector with numerous, vertical line segments.

Within the cleared area, based on interpretations of the radar profiles taken at the 24 observation points, the average depth to the fragipan was 0.75 meter with a range of 0.71 to 0. 87 meters. One-half of the observations had depths to fragipan between 0.72 and 0.78 meters. Based on radar interpretations, depths to fragipan were essentially invariable across the site. Figure 17 shows the interpreted depths to fragipan across the cleared area of the Santa site. The isoline interval is 0.1 meter. Patterns are nondescript.

Figure 18 is the topography of the grid located in the forested area. Relief is 12.92 meters. The surface slopes towards the west. The site is characterized by plane slopes with plane to slightly concave contours.

Figures 19 and 20 are two-dimensional plots of the data collected with the EM38 meter in the forested area. Figures 19 and 20 are simulations based on measurements obtained in horizontal and vertical dipole orientations, respectively. In each plot the interval is 4 mS/m. Comparing the two plots, values of apparent conductivity increased and become slightly more variable with increasing observation depths. In both plots, spatial patterns indicate increasing conductivity towards the lower-lying, northwest corner of the forested area. This trend could reflect increased moisture and clay contents on lower-lying slope positions. However, this interpretation needs to be confirmed by auger observations.

In the forested area, measurements averaged 7.71 mS/m and 12.14 mS/m in the horizontal and vertical dipole orientations, respectively. For the shallower-sensing horizontal dipole orientation, one-half of the observations had values of apparent conductivity between 6.1 and 8.6 mS/m. For the deeper-sensing vertical dipole orientation, one-half of the observations had values of apparent conductivity between 10.0 and 13.5 mS/m. This trend is believed to reflect increased moisture and clay contents at intermediate and lower soil depths.

A comparison was made between the EMI measurements collected at two study areas. Values were higher and less variable in the cleared area. Measurements collected in the cleared area with the EM38 meter in horizontal dipole orientation were the least variable. These measurements could reflect differences in management (application of fertilizer and herbicides in the cleared area).

Because of the dense understory and the number of felled trees, no radar survey was conducted within the forested plot.

Reggear Site:

Two rectangular grids were established across the site. One grid was in a cleared area; one grid was located in a forested area. For each grid, the interval was 5 meters. This interval provided twenty grid intersections or observation points. At each observation point, measurements were taken with an EM38 meter in both the horizontal and vertical dipole orientations. For each measurement, the meter was placed on the ground surface. At each observation point, the relative elevation of the surface was determined with a level and stadia rod. Elevations were not tied to a benchmark; the lowest observation point served as the 0.0 meter datum.

Basic statistics for the EMI data collected within the Reggear site are displayed in Table 3. In both the cleared and forested areas, values of apparent conductivity increased and became more variable with increasing observation depths.

Table 3

Basic Statistics
EMI Survey
Reggear Site
(All values are in mS/m)

CLEARED AREA

				Quartiles			
Meter	**Orientation**	**Minimum**	**Maximum**	**1st**	**Median**	**3rd**	**Average**
EM38	Horizontal	3.3	6.9	4.5	4.8	5.5	5.02
EM38	Vertical	6.4	8.7	6.7	7.1	7.6	7.25

FORESTED AREA

				Quartiles			
Meter	**Orientation**	**Minimum**	**Maximum**	**1st**	**Median**	**3rd**	**Average**
EM38	Horizontal	2.9	8.0	4.0	4.5	4.9	4.56
EM38	Vertical	4.0	9.3	4.8	5.2	5.8	5.44

Figure 21 is a three-dimensional plot of the topography of the cleared area. Relief is 7.34 meters. In general, the surface slopes towards the northeast corner of the study area. The site is characterized by plane slopes with slightly concave contours.

Figures 22 and 23 are two-dimensional plots of the data collected with the EM38 meter in the cleared area. Figures 22 and 23 are simulations based on measurements obtained in horizontal and vertical dipole orientations, respectively. In each plot the interval is 2 mS/m. The spatial patterns appearing in these plots are nondescript. Values of apparent conductivity are invariable across the cleared area. However, these values do increase and become slightly more variable with increasing observation depths.

In the cleared area, measurements averaged 5.02 mS/m and 7.25 mS/m in the horizontal and vertical dipole orientations, respectively. For the shallower-sensing horizontal dipole orientation, one-half of the observations had values of apparent conductivity between 4.5 and 5.5 mS/m. For the deeper-sensing vertical dipole orientation, one-half of the observations had values of apparent conductivity between 6.7 and 7.1 mS/m. This trend is believed to reflect slight increases in moisture and clay contents at intermediate and lower soil depths.

Figure 24 is a three-dimensional plot of the topography of the forested area. Relief is 5.43 meters. In general, the surface slopes towards the north. The site appears to have a slightly irregular, cradle knoll micro-relief.

Figures 25 and 26 are two-dimensional plots of the data collected with the EM38 meter in the forested area. Figures 25 and 26 are simulations based on measurements obtained in horizontal and vertical dipole orientations, respectively. In each plot the interval is 2 mS/m. In both plots, the highest measurements were obtained in a shallow basin near the northeast corner of the study area. Otherwise, spatial patterns appearing in these plots are nondescript. Values of apparent conductivity

are invariable across the remainder of the forested area, but increase slightly with increasing observation depths.

In the forested plot, measurements averaged 4.56 mS/m and 5.44 mS/m in the horizontal and vertical dipole orientations, respectively. For the shallower-sensing horizontal dipole orientation, one-half of the observations had values of apparent conductivity between 4.0 and 4.9 mS/m. For the deeper-sensing vertical dipole orientation, one-half of the observations had values of apparent conductivity between 4.8 and 5.8 mS/m. The similarities between these sets of measurements can be attributed to tree-throw activity and greater soil mixing in this forested area.

A comparison of the EMI data collected within the two areas, revealed slightly higher values in the cleared area. The difference in conductivity between the cleared and forested areas is believed to reflect differences in management (application of fertilizer and herbicides). For each area, values of apparent conductivity were relatively invariable but did increase slightly with increasing observation depths.

Figure 27 is a composite of two radar profiles; one from the cleared area and one from the forested area of the Reggear site. The vertical lines appearing at the top of the radar profile represent the locations of grid intersections. Radar images are noticeably different in the two profiles. The fragipan (immediately below “A” in each profile) appears more irregular and broken in the profile from the forested area. This could reflect the greater tree throw and rooting activities in the forested area. In the cleared area, though typically of lower amplitude, reflections from the fragipan appear to be more continuous and slightly less variable in depth. In addition, the albic horizon (immediately above “A” in each profile) appears to be better expressed in the forested area. In the forested area, the greater signal amplitude of the A/E and the E/Bx interfaces could represent reflections from more contrasting and better developed materials. In both areas, compared with the fragipan, the albic horizon appears more discontinuous and slightly more variable in expression. The fragipan is characterized by intermediate to very strong, nearly continuous, horizontal reflectors. However, unlike the Troy and Santa sites, the fragipan within the Reggear site lacks the conspicuous and often numerous, vertical line segments.

Within the cleared area of the Reggear site, based on interpretations made at 20 observation points on the radar profiles, the average depth to the fragipan was 0.72 meter. The fragipan ranged in depth from 0.67 to 0.78 meters. One-half of the observations had depths to fragipan between 0.68 and 0.72 meters. Based on radar interpretations, depths to fragipan were essentially invariable across the site. Figure 28 shows the interpreted depths to fragipan across the cleared area of the Reggear site. The isoline interval is 0.1 meter. Patterns are nondescript.

Within the forested area of the Reggear site, based on interpretations of the radar profiles taken at the 20 observation points, the average depth to the fragipan was 0.75 meter. The fragipan ranged in depth from 0.57 to 0.89 meters. One-half of the observations had depths to fragipan between 0.72 and 0.79 meters. Based on radar interpretations, depths to fragipan were essentially invariable across the forested area. However, compared with the cleared area, depths were slightly more variable within the forested area. Figure 29 shows the interpreted depths to fragipan across the forested area of the Reggear site. The isoline interval is 0.1 meter. Within the forested area, spatial patterns are more intricate than in the cleared area. Patterns could indicate the effects of greater pedoturbation and possible tree throws.

CONCLUSIONS:

1. Both electromagnetic induction and ground-penetrating radar provided information concerning each site. Variations in electromagnetic induction measurements were slight but did indicate (1) increased conductivity with depth, (2) differences between cleared and forested areas, and (3) difference between sites developed in loess (Troy and Santa) and the site developed in a thin mantle of volcanic ash (Reggear). These differences were assumed to principally reflect (1) variations in clay and moisture

contents with depth, (2) differences induced by dissimilarities in management practices, and (3) contrasts in parent materials.

Ground-penetrating radar provided continuous profiles of subsurface features and conditions. Depths of observation were limited to the upper part of the fragipan. The number of ground-truth observations was limited and, as a consequence, interpretations were not adequately verified. For each site, computer simulations of the depth to fragipan were prepared. The greatest utility of GPR may lie in its ability to capture variations in the expression of the fragipan. Reflection patterns were unique and most intriguing. The expression of this interface changed laterally and with slope position. These patterns could provide soil scientists with insight into the development and expression of fragipans across landscapes.

2. The value of this brief research project probably will not lie in the data collected. This study has demonstrated the utility of two geophysical tools. These tools can be used effectively to collected large amounts of data across vast areas in comparatively short periods of time. Researchers can use the results of this survey to refine the use of these two geophysical tools. Researchers at the University of Idaho are especially encouraged to explore the unique and variable graphic signatures of the fragipan. These signatures may provide a better understanding of the development and expressions of fragipans across landscapes.

It was my pleasure to work with the fine staff of NRCS, ISCC, and the University of Idaho. I enjoyed my stay in Idaho, the fellowship with the participants, and the wonderful Idaho scenery. If I can be of further assistance, please do not hesitate to ask.

With kind regards,

James A. Doolittle
Research Soil Scientist

cc:
J. Culver, Supervisory Soil Scientist, USDA-NRCS, National Soil Survey Center, Federal Building, Room 152,100 Centennial Mall North, Lincoln, NE 68508-3866
S. Holzhey, Supervisory Soil Scientist, USDA-NRCS, National Soil Survey Center, Federal Building, Room 152, 100 Centennial Mall North, Lincoln, NE 68508-3866
P. McDaniel, University of Idaho, Moscow, ID
N. Petersen, State Soil Specialist, USDA-NRCS, Boise, ID
C. MaGrath, State Soil Scientist/MO Leader, USDA-NRCS, Portland, OR

REFERENCES

Ammons, J. T., M. E. Timpson, and D. L. Newton. 1989. Application of aboveground electromagnetic conductivity meter to separate Natraqualfs and Ochraqualfs in Gibson County, Tennessee. Soil Survey Horizons 30(3):66-70.

Arcone, S. 1982. Radar detection of ground water. p. 68-76. *IN:* Dardeau, E. A. (ed.) Proceedings of the Ground-Water Detection Workshop. 12-14 January 1982. Vicksburg, Mississippi. Department of the Army. Waterways Experiment Station.

Collins, M. E., and J. A. Doolittle. 1987. Using ground-penetrating radar to study soil microvariability. Soil Sci. Soc. Am. J. 51:491-493.

Collins, M. E., J. A. Doolittle, and R. V. Rourke. 1989. Mapping depth to bedrock on a glaciated landscape with ground-penetrating radar. Soil Science Society of America J. 53:1806-1812.

Collins, M. E., G. W. Schellentrager, J. A. Doolittle, and S. F. Shih. 1986. Using ground-penetrating radar to study changes in soil map unit composition in selected Histosols. Soil Science Society of America J. 50:408-412.

Cook, P. G., M. W. Hughes, G. R. Walker, and G. B. Allison. 1989. The calibration of frequency-domain electromagnetic induction meters and their possible use in recharge studies. Journal of Hydrology 107:251-265.

Cook, P. G. and G. R. Walker. 1992. Depth profiles of electrical conductivity from linear combinations of electromagnetic induction measurements. Soil Sci. Soc. Am. J. 56:1015-1022.

Corwin, D. L., and J. D. Rhoades. 1982. An improved technique for determining soil electrical conductivity-depth relations from above-ground electromagnetic measurements. Soil Sci. Soc. Am. J. 46:517-520.

Corwin, D. L., and J. D. Rhoades. 1984. Measurements of inverted electrical conductivity profiles using electromagnetic induction. Soil Sci. Soc. Am. J. 48:288-291.

Corwin, D. L., and J. D. Rhoades. 1990. Establishing soil electrical conductivity - depth relations from electromagnetic induction measurements. Communications in Soil Sci. Plant Anal. 21(11&12):861-901.

Daniels, D. J., D. J. Gunton, and H. F. Scott. 1988. Introduction to subsurface radar. IEE Proceedings 135F(4):278-320.

Doolittle, J. A. 1987. Using ground-penetrating radar to increase the quality and efficiency of soil surveys. *IN:* Soil Survey Techniques, Soil Science Society of America Special Publ. No 20. p. 11-32.

Doolittle, J. A. and L. E. Asmussen. 1992. Ten years of applications of ground-penetrating radar by the United States Department of Agriculture. p. 139-147. IN: Hanninen, P. and S. Autio (eds.) Fourth International Conference on Ground Penetrating Radar. June 8-13, 1992. Rovaniemi, Finland. Geological Survey of Finland, Special Paper 16. pp. 365.

Doolittle, J. A., M. A. Hardisky, and M. F. Gross. 1990. A ground-penetrating radar study of active layer thicknesses in areas of moist sedge and wet sedge tundra near Bethel, Alaska, U.S.A. Arctic and Alpine Research 22(2):175-182.

Doolittle, J., R. Murphy, G. Parks, and J. Warner. 1996. Electromagnetic induction investigations of a soil delineation in Reno County, Kansas. Soil Survey Horizons 37:11-20.

Doolittle, J. A., K. A. Sudduth, N. R. Kitchen, and S. J. Indorante. 1994. Estimating depth to claypans using electromagnetic inductive methods. J. Soil and Water Conservation 49(6):552-555.

Farrish, K. W., J. A. Doolittle, and E. E. Gamble. 1990. Loamy substrata and forest productivity of sandy glacial drift soils in Michigan. Canadian Journal of Soil Science 70:181-187.

Hoekstra, P., R. Lahti. J. Hild, R. Bates, and D. Phillips. 1992. Case histories of shallow time domain electromagnetics in environmental site assessments. Ground Water Monitoring Review. 12(4):110-117.

Jaynes, D. B., T. S. Colvin, J. Ambuel. 1993. Soil type and crop yield determination from ground conductivity surveys. 1993 International Meeting of American Society of Agricultural Engineers. Paper No. 933552. ASAE, St. Joseph, MI. pp. 6.

Jaynes, D. B. 1996. Electromagnetic induction as a mapping aid for precision farming. p. 153-156. *IN:* Conference Proceedings. Clean Water, Clean Environment, 21st Century: Team Agriculture. Working to Protect Water Resources. Kansas City, Missouri. March 5-8, 1995.

McBride, R. A., A. M. Gordon, and S. C. Shrive. 1990. Estimating forest soil quality from terrain measurements of apparent electrical conductivity. Soil Sci. Soc. Am. J., 54:290-293.

McNeill, J. D. 1980a. Electromagnetic terrain conductivity measurement at low induction numbers. Technical Note TN-6. Geonics Limited, Mississauga, Ontario. pp. 15.

McNeill, J. D. 1980b. Electrical Conductivity of soils and rocks. Technical Note TN-5. Geonics Ltd., Mississauga, Ontario. pp. 22.

McNeill, J. D. 1986. Geonics EM38 ground conductivity meter operating instructions and survey interpretation techniques. Technical Note TN-21. Geonics Ltd., Mississauga, Ontario. pp. 16.

Mokma, D. L., R. J. Schaetzl, J. A. Doolittle, and E. P. Johnson. 1990a. Ground-penetrating radar study of ortstein continuity in some Michigan Haplaquods. Soil Science Society of America, Journal 54:936-938.

Mokma, D. L., R. J. Schaetzl, E. P. Johnson, and J. A. Doolittle. 1990b. Assessing Bt horizon character in sandy soils using ground-penetrating radar: Implications for soil surveys. Soil Survey Horizons. 30(2):1-8.

Morey, R. M. 1974. Continuous subsurface profiling by impulse radar. p. 212-232. *IN:* Proceedings, ASCE Engineering Foundation Conference on Subsurface Exploration for Underground Excavations and Heavy Construction, held at Henniker, New Hampshire. Aug. 11-16, 1974.

Nettleton, W. D., L. Bushue, J. A. Doolittle, T. J. Endres, and S. J. Indorante. 1994. Sodium-affected soil identification in south-central Illinois by electromagnetic induction. Soil Sci. Soc. Am. J. 58:1190-1193.

Olson, C. G. and J. A. Doolittle. 1985. Geophysical techniques for reconnaissance investigations of soils and surficial deposits in mountainous terrain. Soil Science Society of America J. 49: 1490-1498.

Petroy, D. E. 1994. Assessment of ground-penetrating radar applicability to specific site investigations: Simple methods for pre-survey estimation of likely dielectric constants, target resolution

and reflection strengths. SAGEEP 94. Symposium on the Application of Geophysics to Engineering and Environmental Problems. 27 to 31 March 1994. Boston, Massachusetts. pp. 21.

Puckett, W. E., M. E. Collins, and G. W. Schellentrager. 1990. Design of soil map units on a karst area in West Central Florida. Soil Science Society of America J. 54:1068-1073.

Rhoades, J. D. and D. L. Corwin. 1981. Determining soil electrical conductivity-depth relations using an inductive electromagnetic soil conductivity meter. Soil Sci. Soc. Am. J. 45:255-260.

Rhoades, J. D., N. A. Manteghi, P. J. Shouse, and W. J. Alves. 1989. Soil Electrical conductivity and soil salinity: new formulation and calibrations. Soil Sci. Soc. Am. J. 53:433-439.

Schellentrager, G. W., J. A. Doolittle, T. E. Calhoun, and C. A. Wettstein. 1988. Using ground-penetrating radar to update soil survey information. Soil Science Society of America J. 52:746-752.

Shih, S. F. and J. A. Doolittle. 1984. Using radar to investigate organic soil thickness in the Florida Everglades. Soil Science Society of America J. 48:651-656.

Shih, S. F., J. A. Doolittle, D. L. Myhre, and G. W. Schellentrager. 1986. Using radar for groundwater investigation. J. Irrigation and Drainage Engineering. 112(2):110-118.

Shih, S. F., D. L. Myhre, G. W. Schellentrager, V. W. Carlisle, and J. A. Doolittle. 1985. Using radar to assess the soil characteristics related to citrus stress. Soil and Crop Science of Florida, Proc. 45:54-59.

Slavich, P. G. and G. H. Petterson. 1990. Estimating average rootzone salinity from electromagnetic induction (EMI-38) measurements. Australian J. Soil Res. 28:453-463.

Sudduth, K. A. and N. R. Kitchen, 1993. Electromagnetic induction sensing of claypan depth. Paper No. 93-1550. Presented at the December 1993, Winter Meetings of the American Society of Agricultural Engineers. St. Joseph, Michigan. pp. 18.

Violette, P. 1987. Surface geophysical techniques for aquifers and wellhead protection area delineation. Environmental Protection Agency, Office of Ground Water Protection, Washington, DC, pp. 1-49.

Williams, B. G. and G. C. Baker. 1982. An electromagnetic induction technique for reconnaissance surveys of soil salinity hazards. Australian J. Soil Res. 20:107-118.

Wollenhaupt, N. C., J. L. Richardson, J. E. Foss, and E. C. Doll. 1986. A rapid method for estimating weighted soil salinity from apparent soil electrical conductivity measured with an aboveground electromagnetic induction meter. Can J. Soil Sci. 66:315-321.

SITE 1
TROY, IDAHO
RELATIVE TOPOGRAPHY

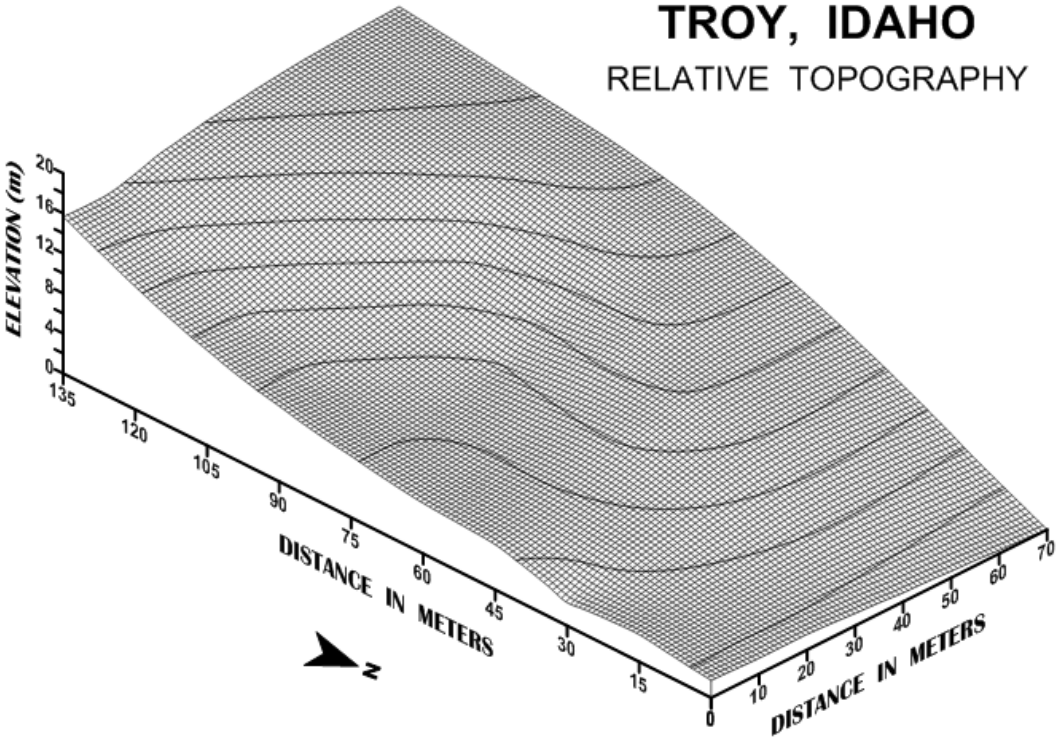

SITE 1
TROY, IDAHO
EM SURVEY
EM38 METER
HORIZONTAL DIPOLE ORIENTATION

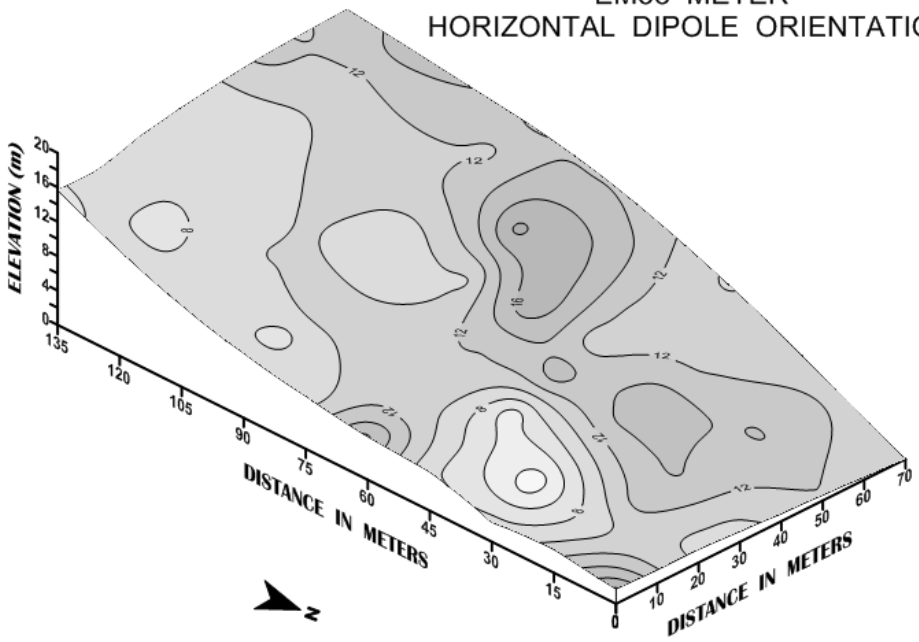

SITE 1
TROY, IDAHO
EM SURVEY
EM38 METER
VERTICAL DIPOLE ORIENTATION

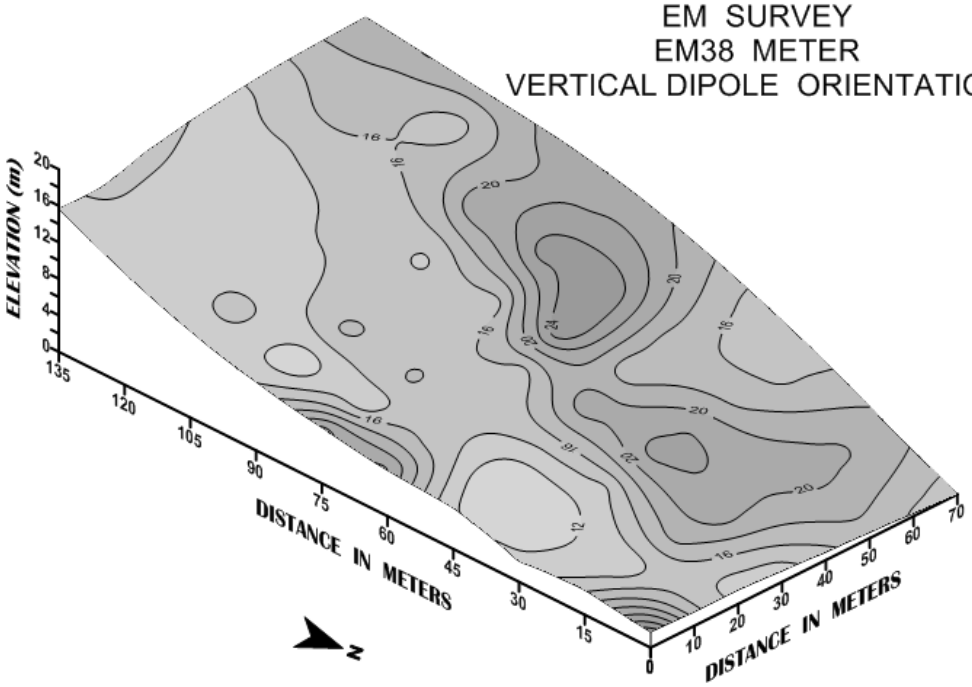

SITE 1
TROY, IDAHO
EM SURVEY
EM31 METER
HORIZONTAL DIPOLE ORIENTATION

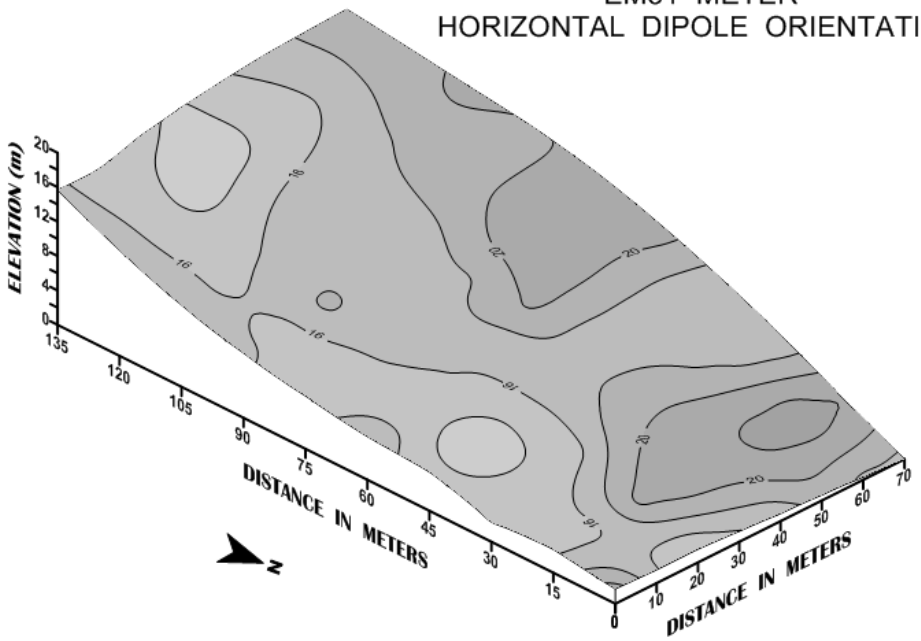

SITE 1
TROY, IDAHO
EM SURVEY
EM31 METER
VERTICAL DIPOLE ORIENTATION

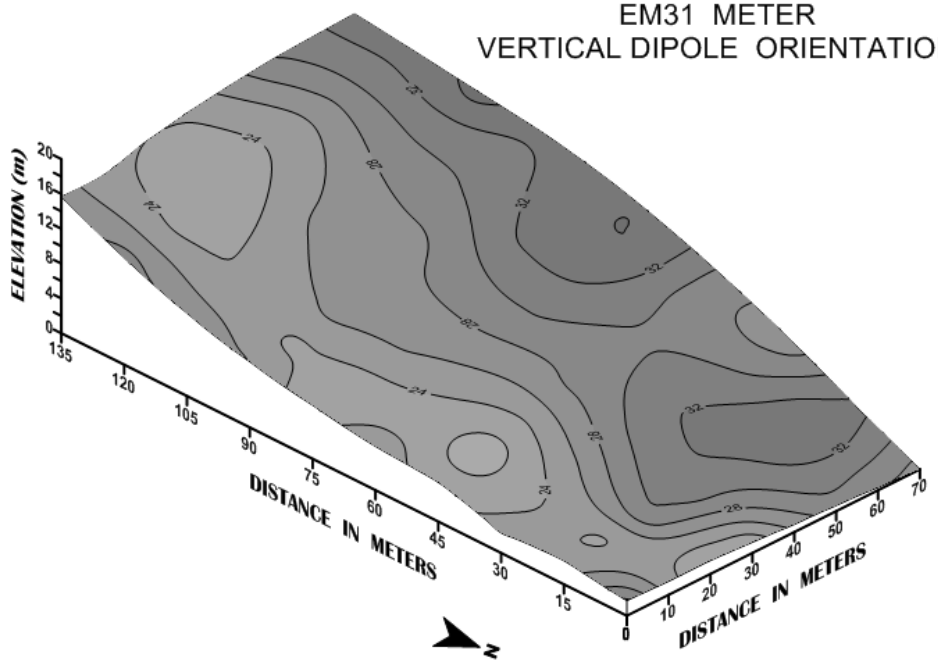

SITE 1
TROY, IDAHO
DEPTH TO FRAGIPAN

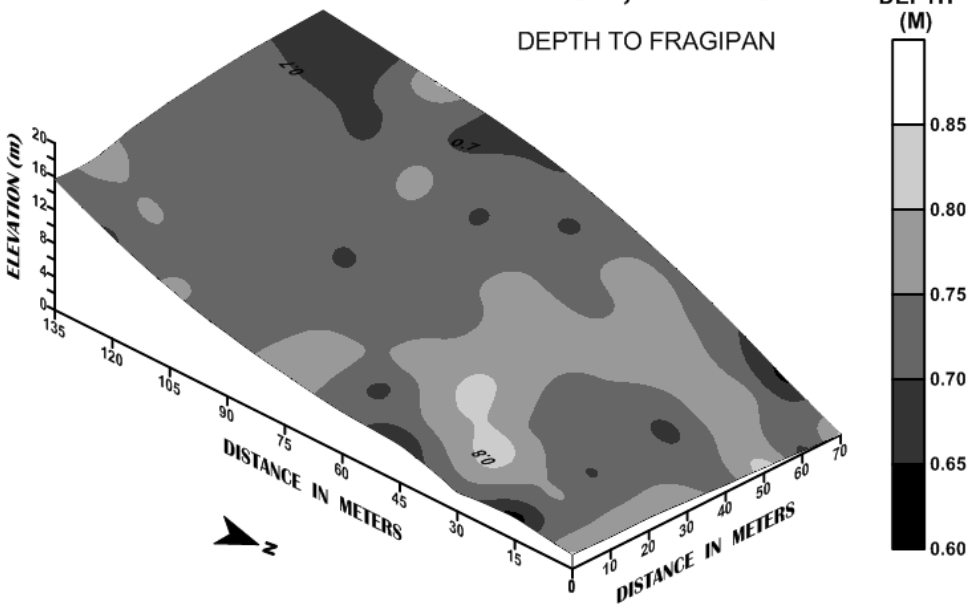

SANTA SITE
TROY, IDAHO

RELATIVE TOPOGRAPHY

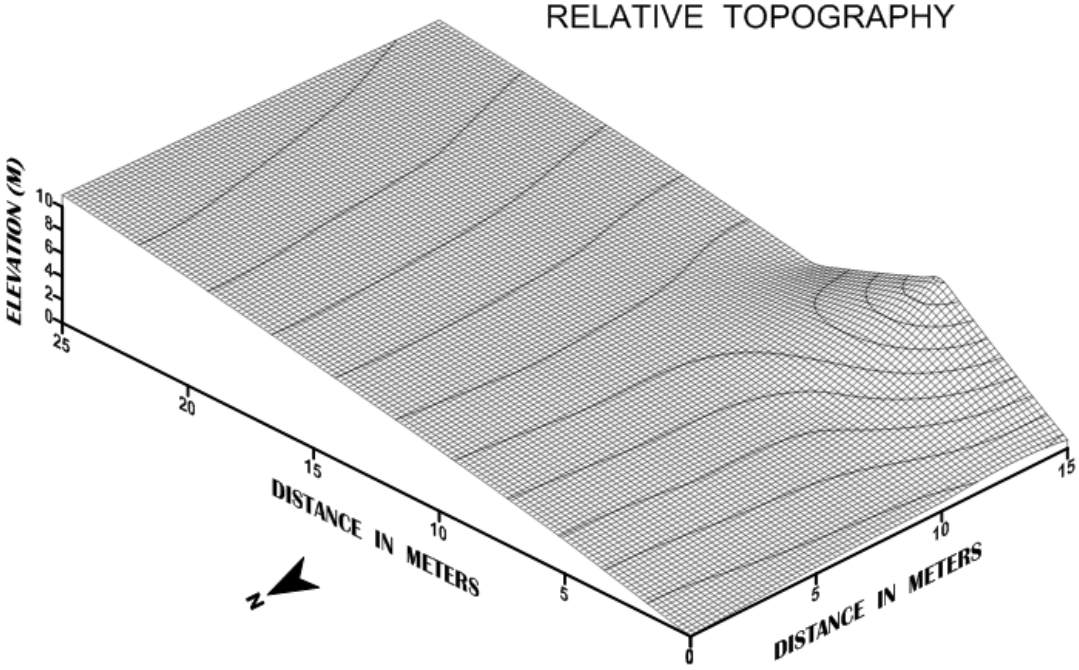

SANTA SITE
TROY, IDAHO

EM SURVEY
EM38 METER
HORIZONTAL DIPOLE ORIENTATION

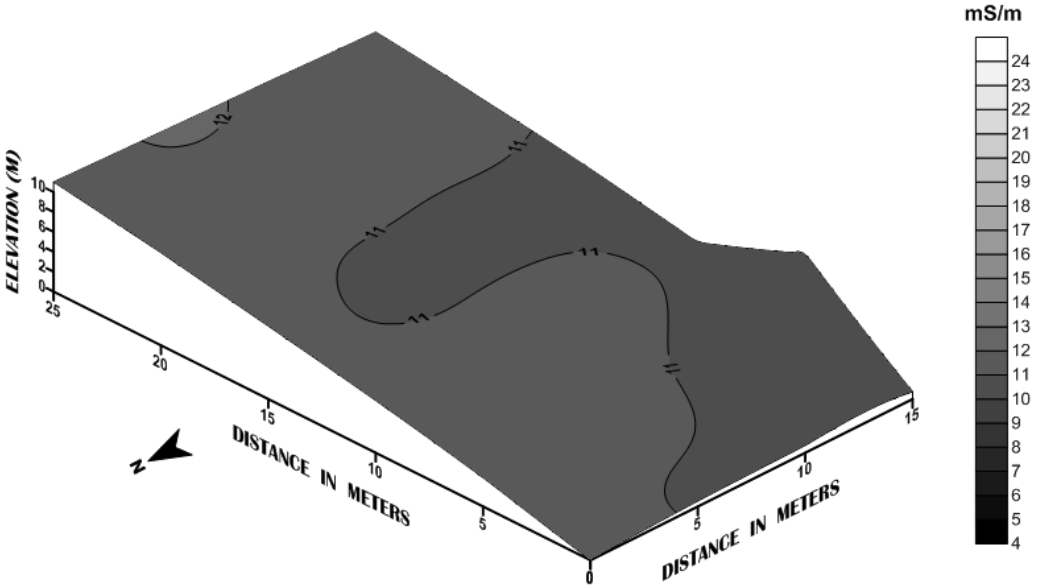

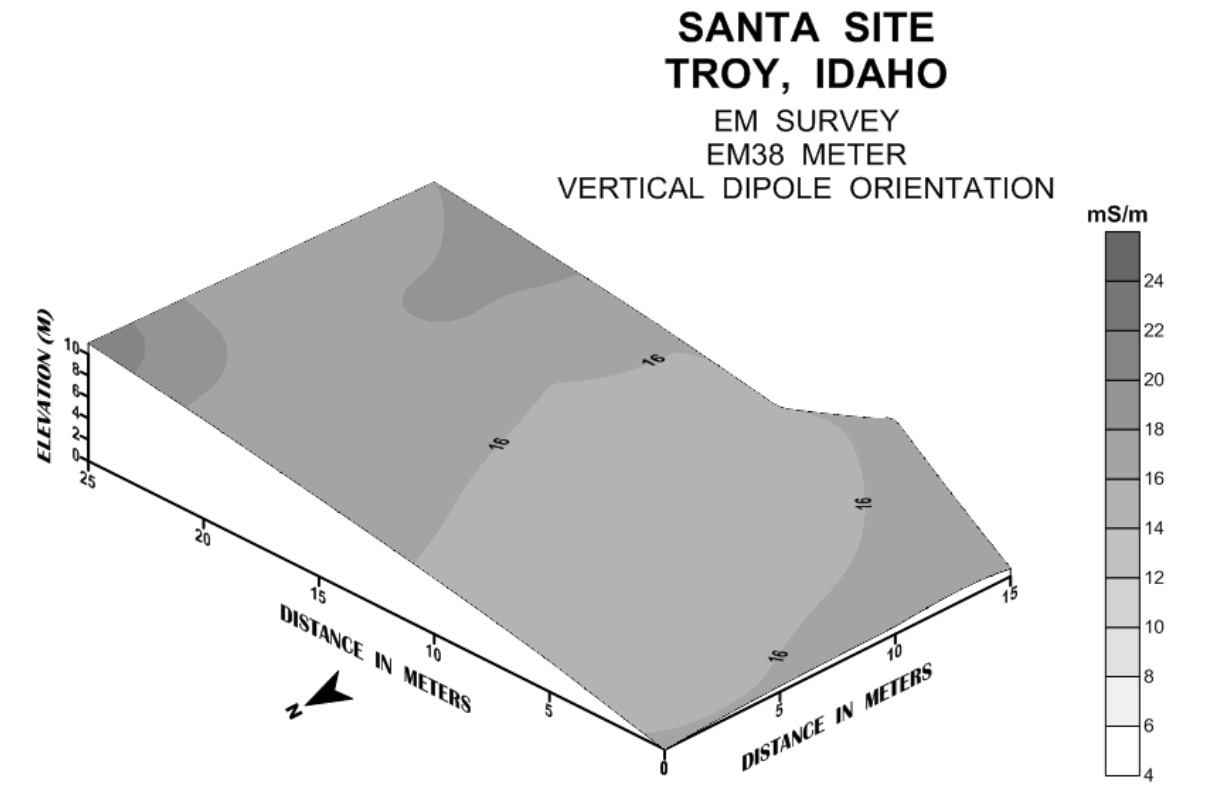
SANTA SITE
TROY, IDAHO
EM SURVEY
EM38 METER
VERTICAL DIPOLE ORIENTATION
mS/m
24
22
20
18
16
14
12
10
8
6
4
ELEVATION (M)
DISTANCE IN METERS
DISTANCE IN METERS
N
16

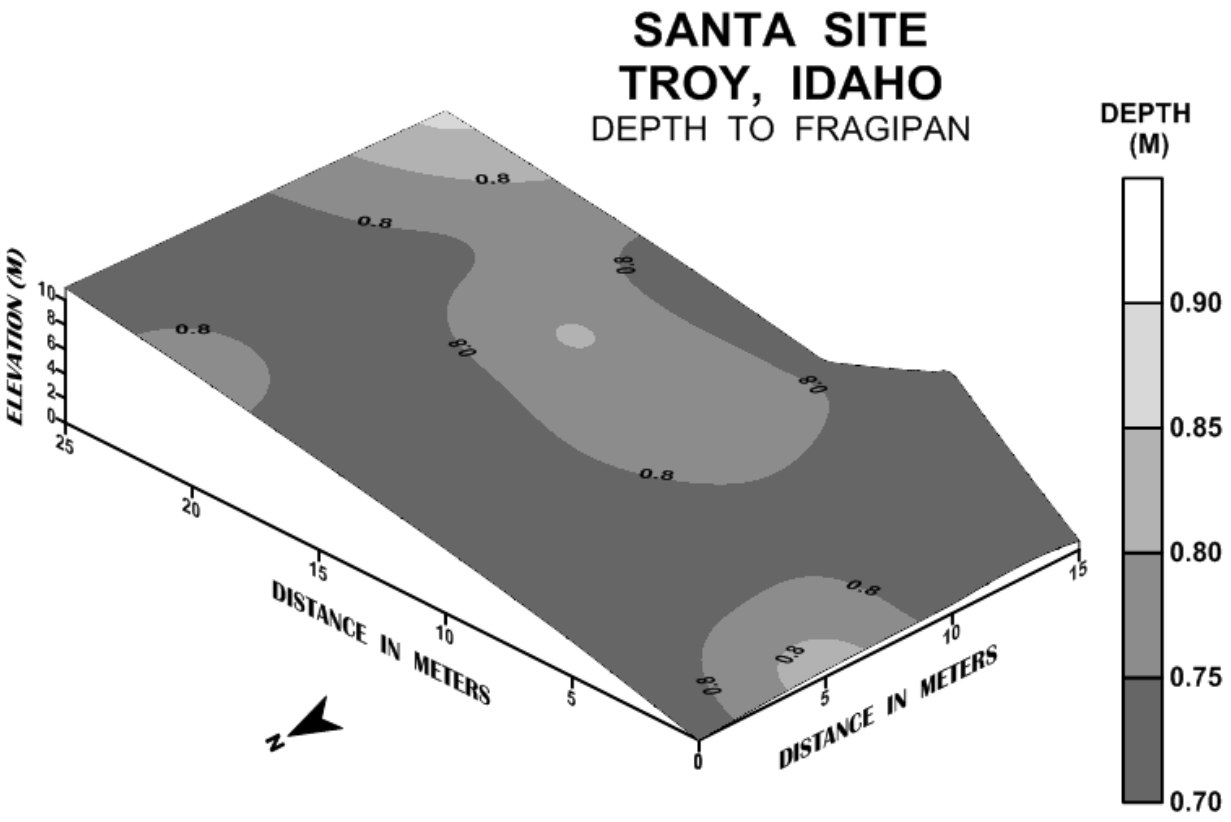
SANTA SITE
TROY, IDAHO
DEPTH TO FRAGIPAN
DEPTH
(M)
0.90
0.85
0.80
0.75
0.70
ELEVATION (M)
DISTANCE IN METERS
DISTANCE IN METERS
N
0.8

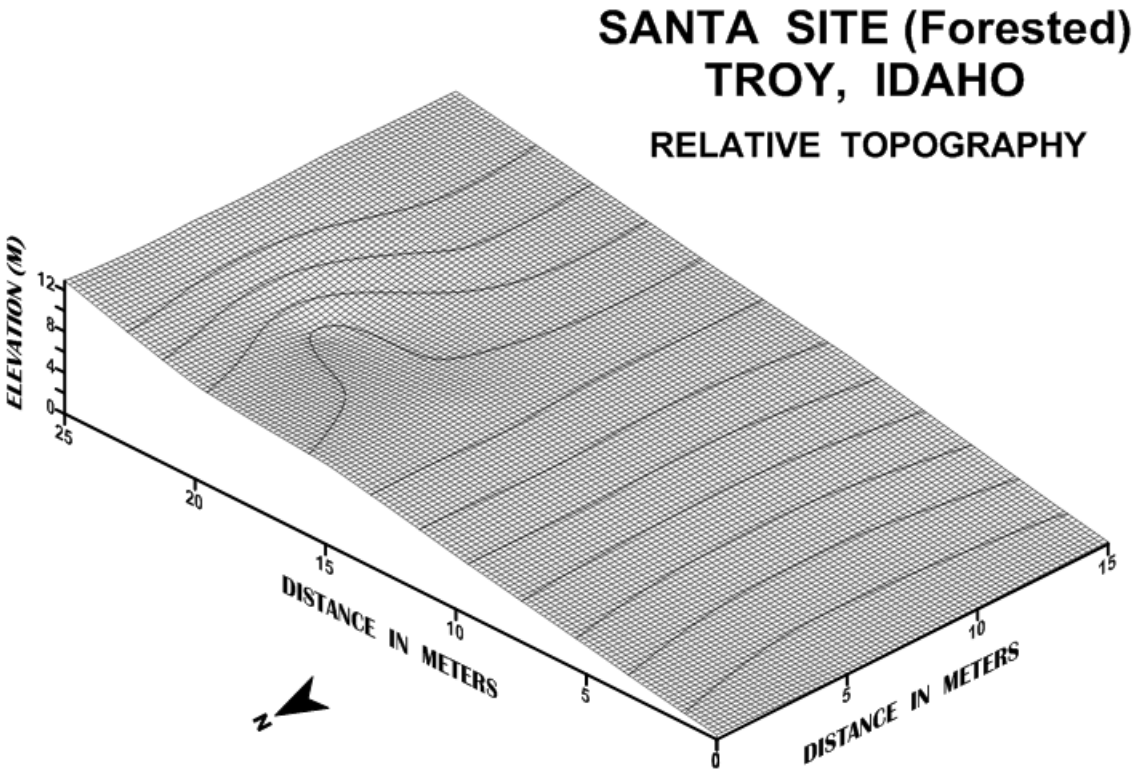
SANTA SITE (Forested)
TROY, IDAHO
RELATIVE TOPOGRAPHY
ELEVATION (M)
12
8
4
0
25
20
15
10
5
0
DISTANCE IN METERS
N
15
10
5
DISTANCE IN METERS

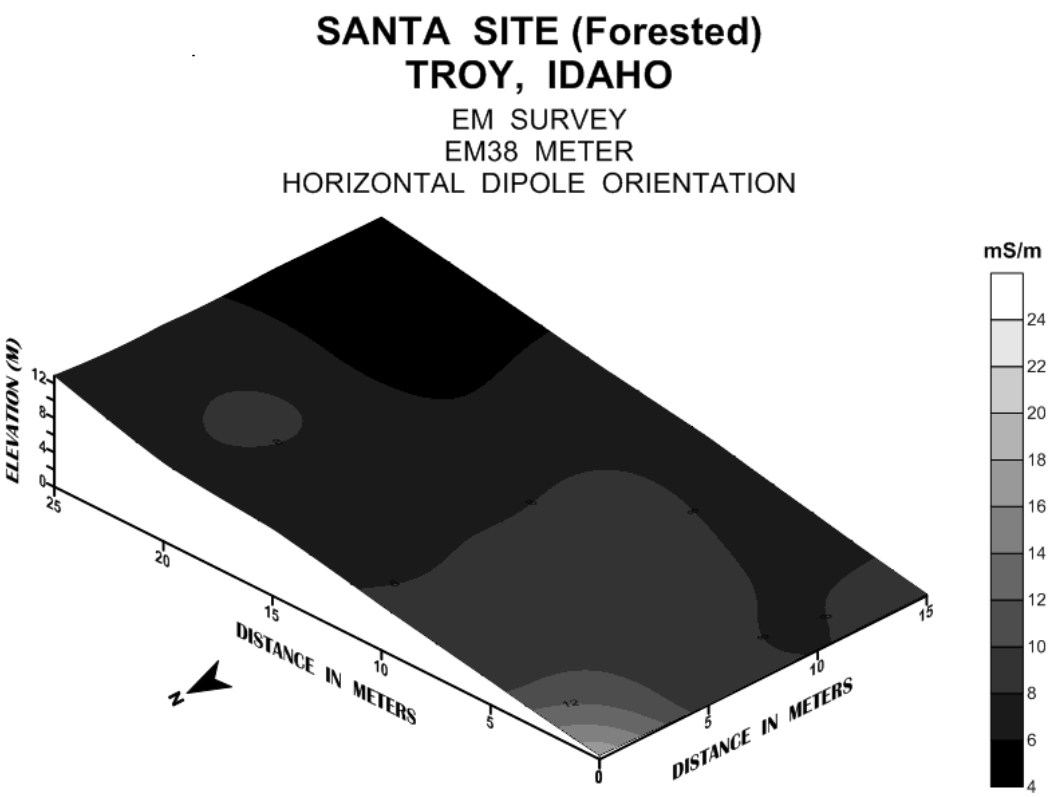
SANTA SITE (Forested)
TROY, IDAHO
EM SURVEY
EM38 METER
HORIZONTAL DIPOLE ORIENTATION
mS/m
24
22
20
18
16
14
12
10
8
6
4
ELEVATION (M)
12
8
4
0
25
20
15
10
5
0
DISTANCE IN METERS
N
15
10
5
DISTANCE IN METERS

SANTA SITE (Forested)
TROY, IDAHO
EM SURVEY
EM38 METER
VERTICAL DIPOLE ORIENTATION

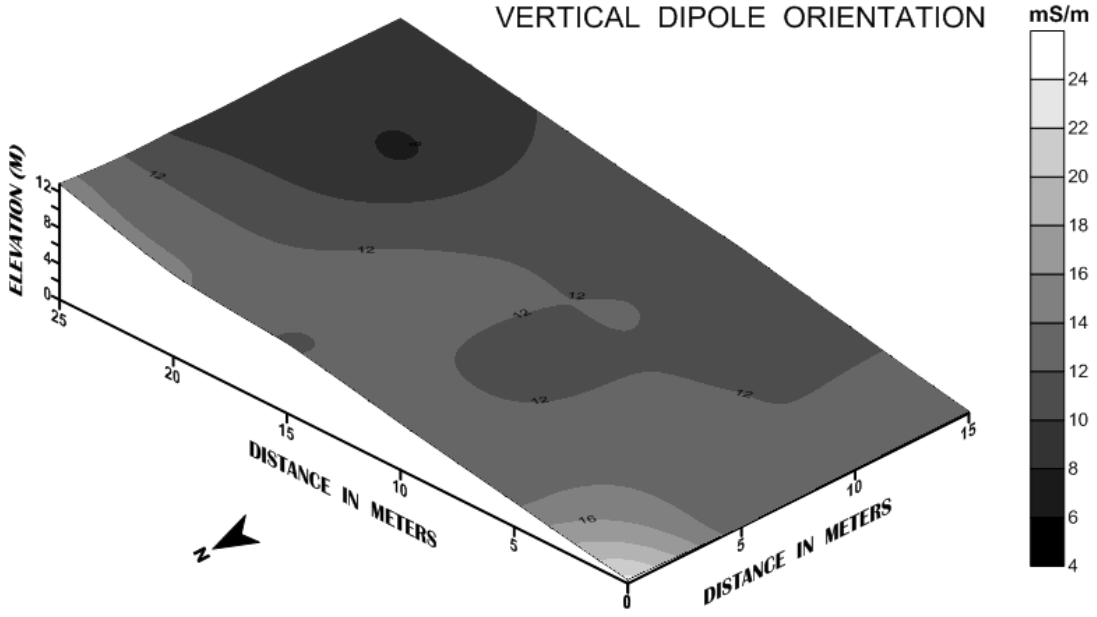

REGGEAR SITE
WEIPPE, IDAHO
RELATIVE TOPOGRAPHY

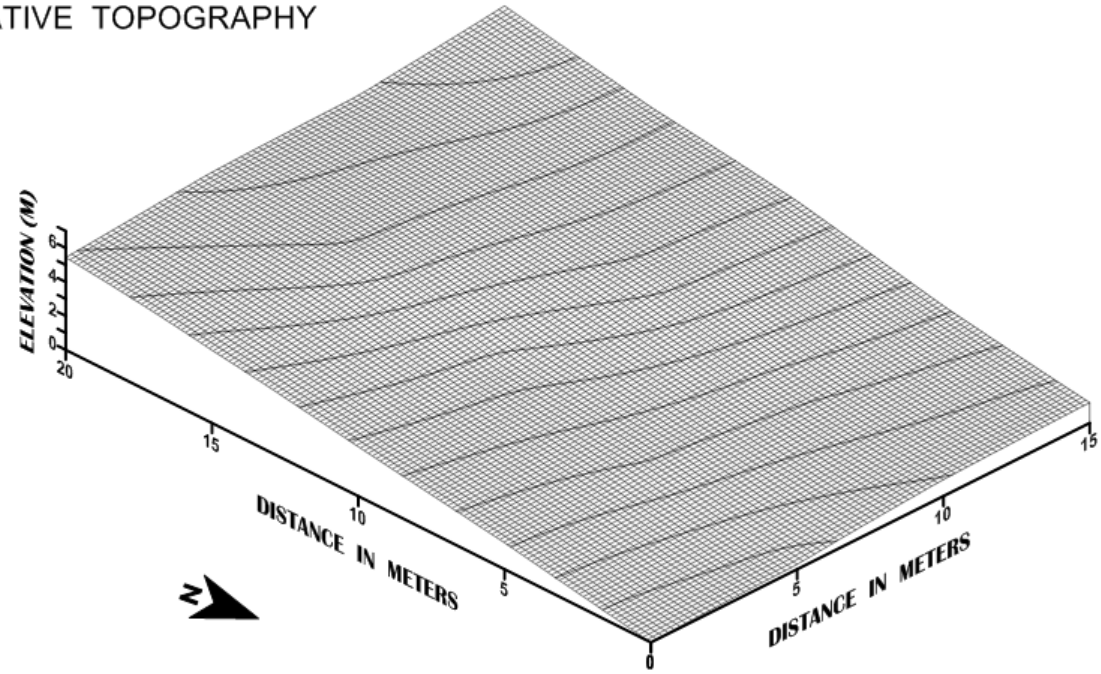

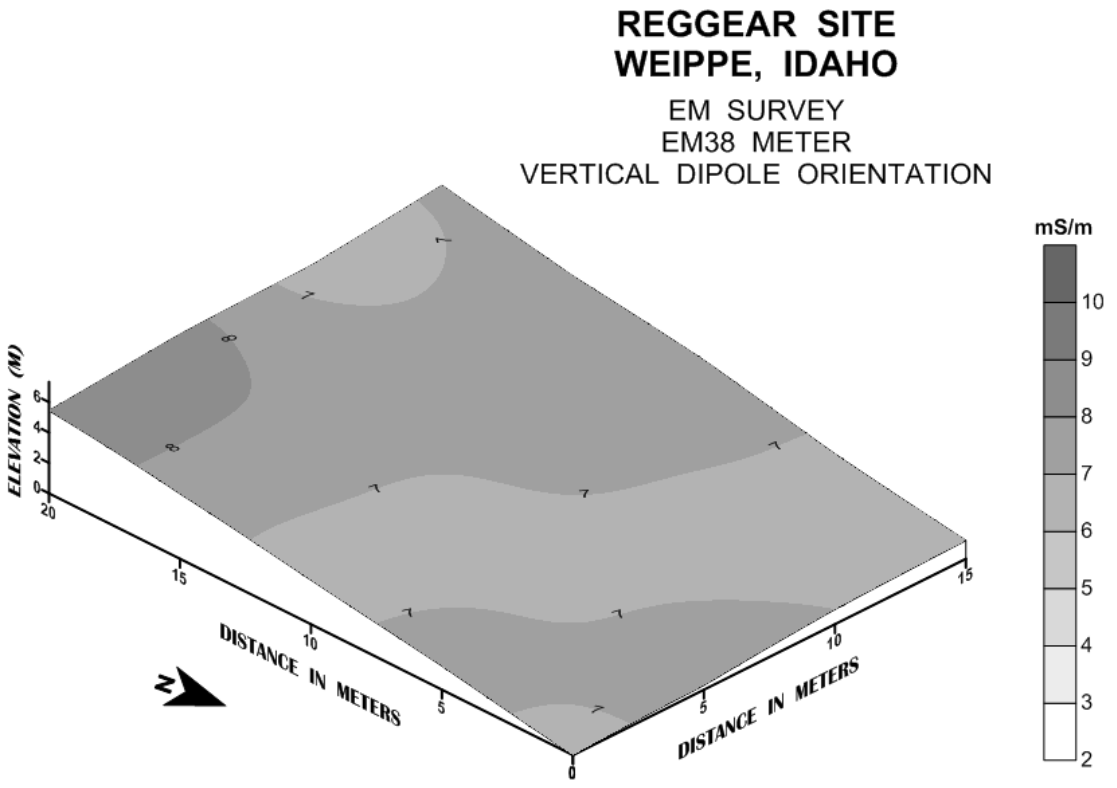
REGGEAR SITE
WEIPPE, IDAHO
EM SURVEY
EM38 METER
VERTICAL DIPOLE ORIENTATION
mS/m
10
9
8
7
6
5
4
3
2
ELEVATION (M)
DISTANCE IN METERS
DISTANCE IN METERS
N

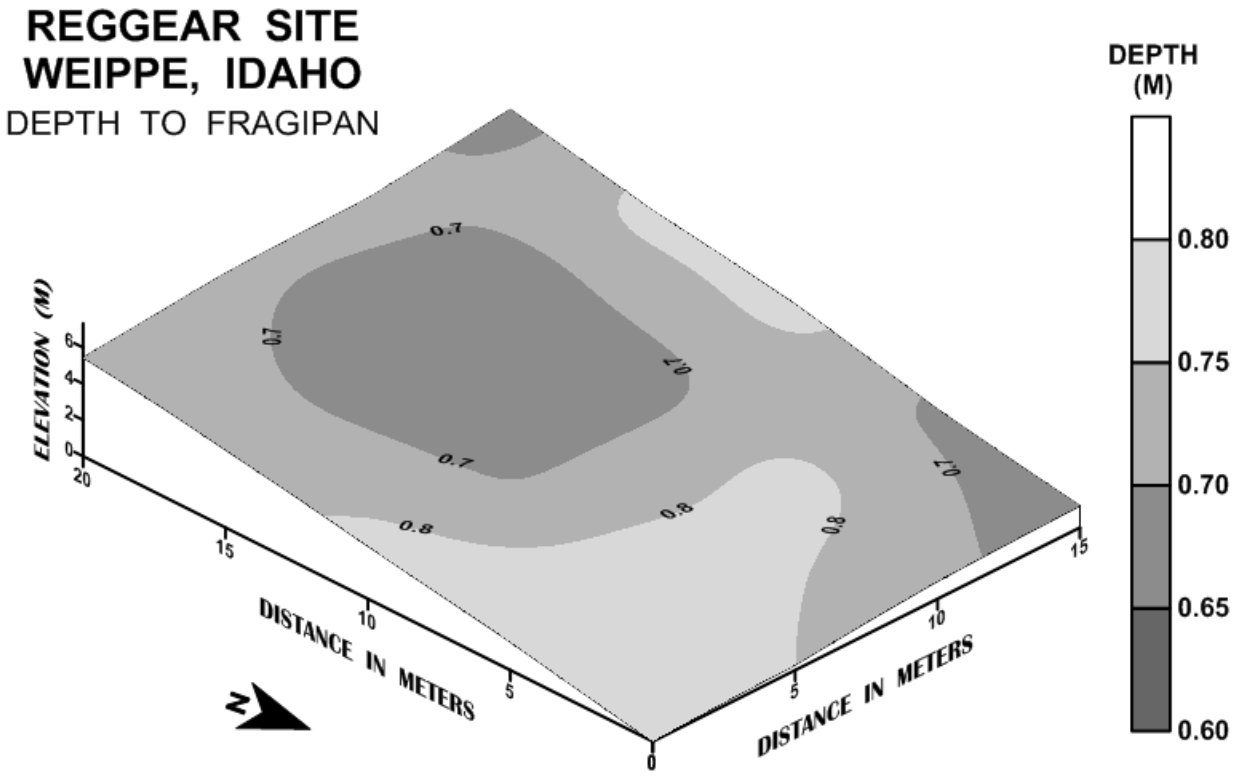
REGGEAR SITE
WEIPPE, IDAHO
DEPTH TO FRAGIPAN
DEPTH
(M)
0.80
0.75
0.70
0.65
0.60
ELEVATION (M)
DISTANCE IN METERS
DISTANCE IN METERS
N

REGGEAR SITE (FORESTED)
WEIPPE, IDAHO
RELATIVE TOPOGRAPHY

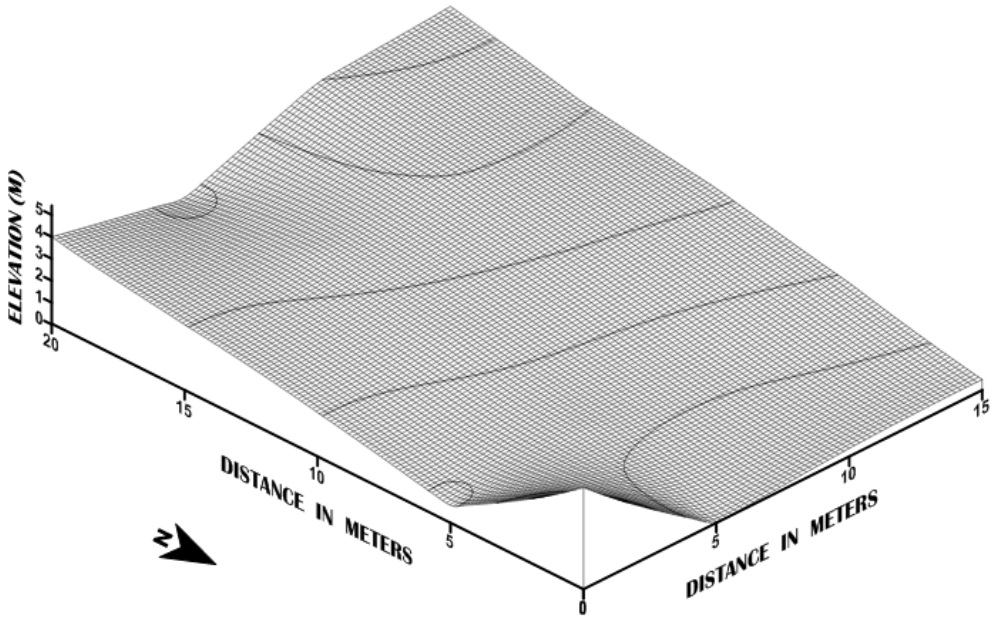

REGGEAR SITE (FORESTED)
WEIPPE, IDAHO
EM SURVEY
EM38 METER
HORIZONTAL DIPOLE ORIENTATION

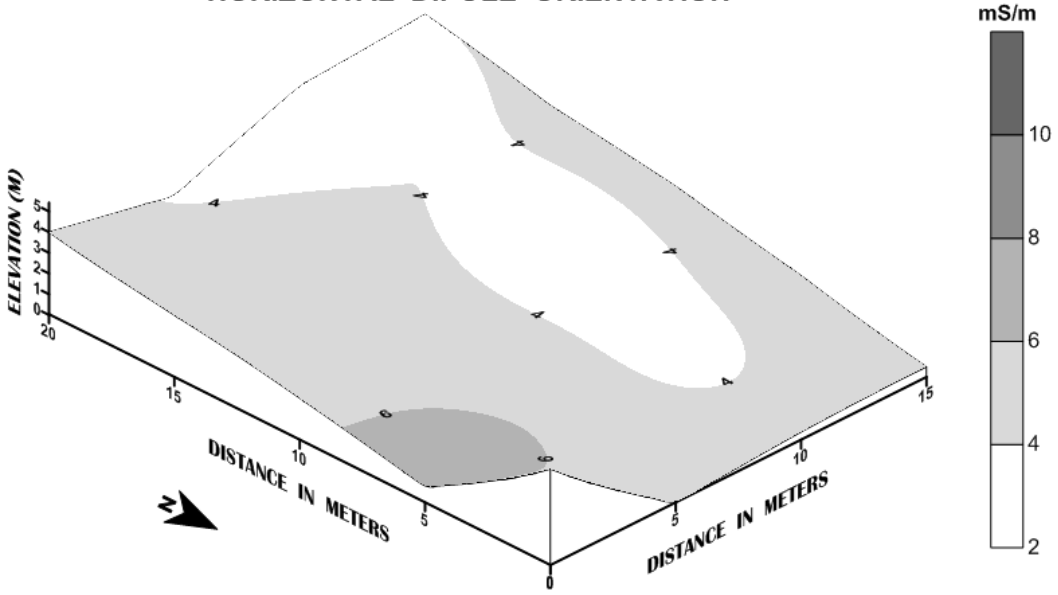

REGGEAR SITE (FORESTED)
WEIPPE, IDAHO
DEPTH TO FRAGIPAN

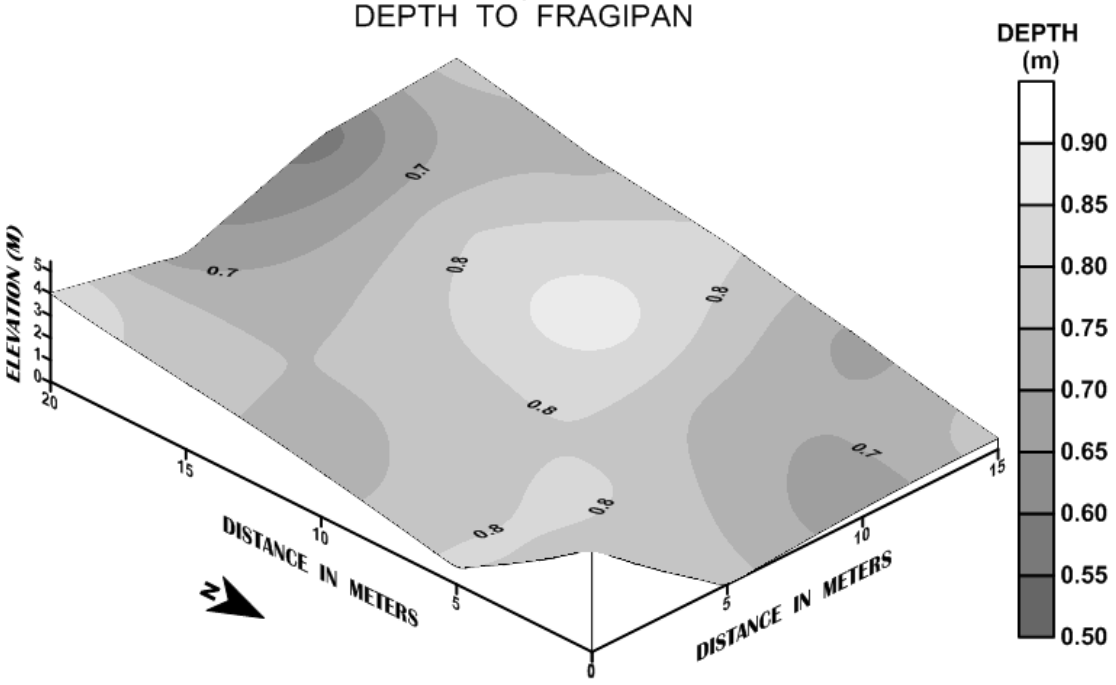

REGGEAR SITE (FORESTED)
WEIPPE, IDAHO
EM SURVEY
EM38 METER
VERTICAL DIPOLE ORIENTATION